# Experimental and CFD modeling of a vortex flow restrictor

**Arturo S. León[1], Yovanni A. Cataño-Lopera[2], Xiaofeng Liu[3], Arthur R. Schmidt[4], Marcelo H. García[5]**

[1] Post-doctoral Research Associate, Dept. of Civil and Envir. Engng., Univ. of Illinois at Urbana-Champaign, 2519 Hydrosystems Lab., MC-250. 205 North Mathews Av., Urbana, IL 61801. E-mail: asleon@uiuc.edu (corresponding author).
[2] Post-doctoral Research Associate, Dept. of Civil and Envir. Engng., Univ. of Illinois at Urbana-Champaign, 2524 Hydrosystems Lab., MC-250. 205 North Mathews Av., Urbana, IL 61801. E-mail: catano@uiuc.edu.
[3] Ph.D student, Dept. of Civil and Envir. Engng., Univ. of Illinois at Urbana-Champaign, 2519 Hydrosystems Lab., MC-250. 205 North Mathews Av., Urbana, IL 61801. E-mail: liu19@uiuc.edu.
[4] Research Assistant Professor, Dept. of Civil and Envir. Engng., Univ. of Illinois at Urbana-Champaign, 2535a Hydrosystems Lab., MC-250. 205 North Mathews Av., Urbana, IL 61801. E-mail: aschmidt@uiuc.edu.
[5] Chester and Helen Siess Professor and Director, Dept. of Civil and Envir. Engng., Univ. of Illinois at Urbana-Champaign, 2535b Hydrosystems Lab., MC-250. 205 North Mathews Av., Urbana, IL 61801. E-mail: mhgarcia@uiuc.edu.

## Abstract

Flow restrictors or rain blockers are devices installed at inlets or manholes to limit storm runoff entering a Combined Sewer System (CSS). One type of these structures is the vortex flow restrictor (VFR). Although a large number of this type of restrictor have been installed in CSSs in urban areas, the authors are not aware of any systematic study on the performance of the VFR in limiting peak flows. Herein the results of an experimental and numerical study of a VFR are presented. For the numerical study, a state-of-the-art three-dimensional Computational Fluid Dynamics (CFD) model was used. The numerical results for the discharge coefficient and rating curves show good agreement with the experimental observations. The results show that the flow discharge passing through a VFR can be reduced substantially compared to the case where no flow restrictor is in place. The results also show that the flow discharge depends strongly on the way the VFR is installed.
**Keywords:** Combined sewer flow; Computational fluid dynamics technique; Grid systems; Sewer System; Three-dimensional models; Vortex Flow restrictor.

## Introduction

Sewer catch basins are chambers used to collect water either from surface inlets or from in-flowing sewer lines. The purpose of the catch basin is to consolidate the inflows and

pass the water downstream via a single outflow pipe. During heavy rains or rapid snow melt, substantial amounts of water are directed into the catch basins and eventually into the main sewer lines. When the incoming flows exceed the capacity of the main sewer lines, pressurization occurs and the branch lines surcharge. Back flows can occur in these situations, which in turn can result in residential flooding. In combined sewer systems, this back flow can have potentially hazardous health consequences for the inhabitants of the flooded neighborhood. Damage costs associated with these events make it imperative that appropriate countermeasures are found to help minimize their occurrence.

Two types of flow restrictors have been used to limit peak flows entering a CSS system - the hanging trap and the VFR. The hanging trap uses a small diameter orifice to limit flow into the outflow pipe. The outlet is elevated off the bottom of a catch basin to allow room for debris to accumulate without clogging the opening. The VFR limits flow by forcing flow through a helicoidal chamber followed by sudden expansions and contractions that create high internal turbulence which in turn produces large head losses. The large head losses produced in a VFR limits flow rates much more than a simple orifice, while maintaining a relatively large flow opening that can reduce the chance of clogging. The VFR is also elevated off the bottom to allow room for debris accumulation. The present paper is limited to VFRs.

Although a large number of VFR have been installed in CSSs in urban areas, to date the authors are not aware of any systematic study on the performance of VFR in limiting peak flows that enter a CSS system. Thus the need to investigate the behavior of these restrictors through physical and numerical experimentation. Herein the results of an experimental and numerical study of a VFR are presented. In particular the discharge coefficients associated with this type of restrictor are presented. These coefficients can be used in hydrologic/hydraulic models for prediction of inflows at sewer-manholes that use this type of flow restrictor.

## Background

A VFR is a device designed to limit peak runoff flows that can be passed from a vertically oriented storm drain structure (e.g. catch basin or manhole) into a generally horizontally oriented storm sewer pipe (Raasch 2002). A perspective view of this restrictor is presented in Fig. 1. A portion of the flow restrictor sits outside of the pipe and consists of a helicoidal chamber and orifice that serve to limit the amount of water allowed to pass into the outflowing sewer pipe, keeping excess storm water runoff on the street for longer periods of time and allowing the residential branch lines to drain freely, thereby minimizing the amount of basement flooding that occurs as a result of sewer back-ups. The restrictor also has a section that is inserted into the outlet pipe. This section is equipped with two rubber seals that are forced to expand when two lugs are tightened and the conical end cap is pulled inward, forcing the expansion of a series of plastic slats. The rubber seals serve the dual purpose of preventing flow from bypassing the orifice of the flow restrictor and anchoring the restrictor in place as the seals radially expand to tightly and frictionally engage an interior surface of the storm sewer pipe (Raasch 2002). As will be shown later, the exact position of the upstream most seal has a large impact on the discharge coefficient. The length, $L_s$, is defined as the distance between the upstream end of the plastic slats and

the location of the upstream seal (Fig. 2). A distance $L_s$ = 0 cm indicates that the seal is completely upstream of the slats and a distance $L_s$ = 7.2 cm indicates that the seal is positioned against the downstream seal, with 7.2 cm of the slats exposed.

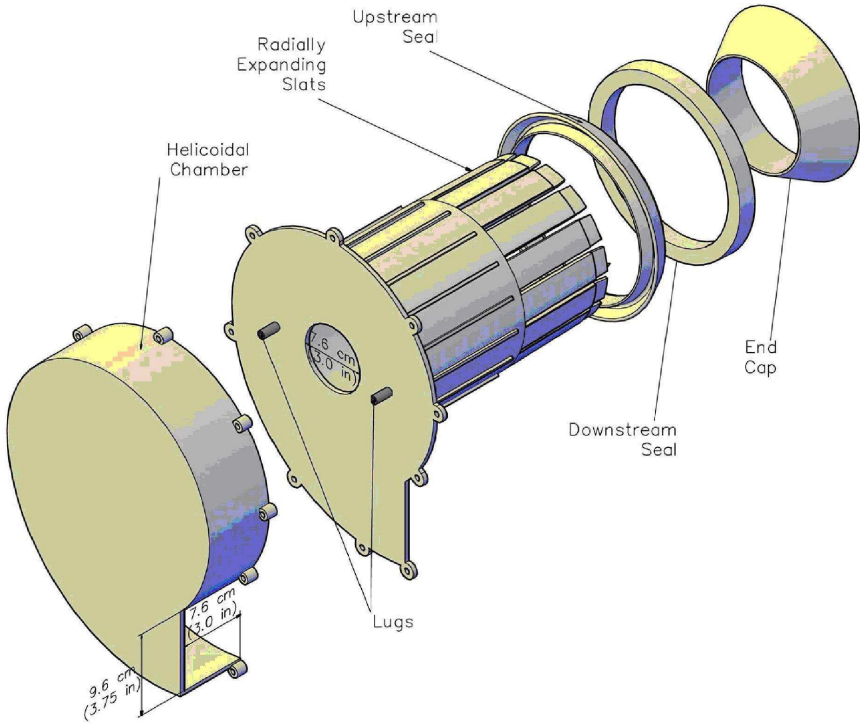


Fig. 1. Perspective view of a vortex flow restrictor

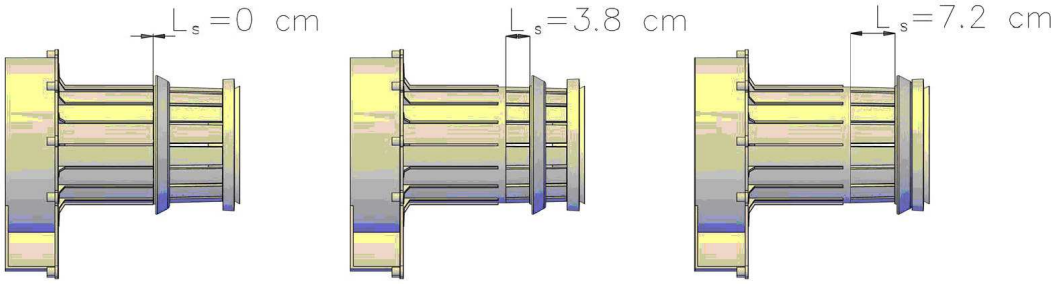


Fig. 2. Sketch of seals position

If a flow-restriction device allows too much discharge to pass onto the downstream sewer main, it may still result in potential sewer backups and subsequent flooding, thereby eliminating the benefit of installing the flow restrictor in the first place. If a device is over-restrictive, it may back up too much water onto the surface, resulting in overland flooding while the sewer mains are still below capacity. Therefore, it is extremely important that a reliable estimate of the discharge coefficient be available for designers to use in their

calculations in order to optimize the operation of the sewer system - thus the purpose of this study.

## Experimental facility and measurements

The experiments were conducted at the Ven Te Chow Hydrosystems Laboratory at the University of Illinois at Urbana-Champaign. The experimental facility consists of a full scale precast manhole prototype which is depicted in Fig. 3(a). The system was fed by a 20.3-cm (8-in) PVC pipe connected to the laboratory constant-head water tank. An electromagnetic flow meter was used to measure the flow discharge in the inlet pipe. This flow meter can measure discharges ranging between 1.7 - 320 l/s with an accuracy if +/- 0.5% of the measured discharge. The 20.3-cm inlet pipe discharged near the bottom of the "manhole tank" [Fig. 3(a)] basin in an attempt to minimize the intensity of flow disturbances at the level of the flow restrictor.

The outflow pipe in Fig. 3(a) was setup in such a way that the flow restrictor always operates under pipe-full (pressurized) flow conditions. This was desirable because it has been shown that the discharge coefficient is dependant upon downstream submergence (Nelson and Weber 2000). By maintaining pipe-full flow conditions, any variability in the discharge coefficient related to backwater conditions in the downstream piping should be eliminated.

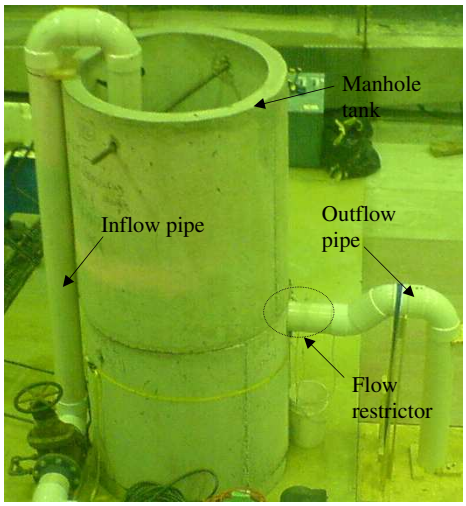


(a) Experimental setup for physical study

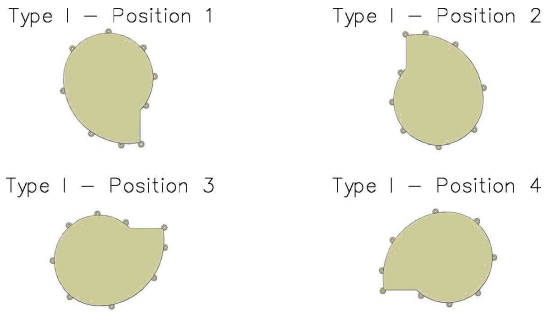


(b) Configurations of VFR

Fig. 3.

Four different positions of the VFR were tested in the experiments [Fig. 3(b)]. These positions were obtained by rotating the VFR 90 degrees. The physical study was conducted using three configurations, however in this paper only two configurations are presented. In the first configuration, the VFR is not used. In the second configuration, the VFR is placed into the outflow pipe [Fig. 3(a)]. For the second configuration nine experiments were performed: three tests with the restrictor in position 1 ($L_s$ = 0 cm, $L_s$ = 3.8 cm, $L_s$ = 7.2 cm (Fig. 2), and two each with the restrictor in positions 2, 3 and 4 ($L_s$ = 0 cm and $L_s$ = 7.2 cm). The variables measured were the flow discharge $Q$, the piezometric head at the

manhole tank ($H_t$) and the piezometric head right downstream of the VFR ($H_v$).

The head loss coefficient ($k$) associated with the VFR in steady flow conditions can be estimated using the following relationship

$$h_f = k\frac{\overline{v}^2}{2g} \tag{1}$$

where $h_f$ is the head loss associated to the VFR, $\overline{v}$ is an average flow velocity, and $g$ is the gravitational acceleration constant. $h_f$ can be obtained from the experiments as $h_f = H_t - H_v$, and from Eq. (1) only $\overline{v}$ need to be determined for computing $k$. The calculation of $\overline{v}$ should be based upon the controlling cross-sectional area. For the VFR, the controlling cross-sectional area is the rectangular entrance to the VFR (72.58 cm$^2$). The non-dimensional discharge coefficient ($C_d$) can be related to $k$ by

$$C_d = \sqrt{\frac{1}{k}} \tag{2}$$

## Numerical Modeling

The numerical study was performed using the commercially available CFD package FLOW-3D (Flow Science 2005), a state-of-the-art three-dimensional CFD model. FLOW-3D uses the finite-volume method to solve the Reynolds-Averaged Navier-Stokes (RANS) equations. The computational domain is subdivided using Cartesian coordinates into a grid of variable-sized hexahedral cells. For each cell, average values for the flow parameters (pressure and velocity) are computed at discrete times using a staggered grid technique (Versteeg and Malalasekera 1995). The $k-\varepsilon$ model, as outlined by Rodi (1980), was used for turbulence closure. To represent obstacles FLOW-3D uses the Fractional Area/Volume Obstacle Representation (FAVOR) method, which is outlined by Hirt and Sicilian (1985) and Hirt (1992). The FAVOR method is a porosity technique with a value of zero within obstacles and 1 for cells without the obstacle. Cells only partially filled with an obstacle have a value between zero and 1, based on the percent volume that is solid.

### *Numerical Model Implementation*

Two configurations were adopted in the numerical simulations (Fig. 4). The first configuration consisted of a cylindrical manhole tank with an inlet pipe as in the physical model Fig. 3(a). In this configuration, a velocity boundary condition was specified at the beginning of the inlet pipe. The second configuration did not include a cylindrical tank, but a rectangular open pool, so that a pressure boundary condition can be specified. The simulations to achieve steady state using the first configuration were found to be computationally much more demanding than the second one. However, the results achieved in two different simulations by using the two configurations were found to be very similar (a difference of less than 2%). Thus, the second configuration was adopted in all simulations.

The thickness of the VFR and the outlet pipe were increased to be able to represent their walls with a smaller number of cells. To speed up convergence, a multi-block gridding technique was implemented, which is presented in Fig. 5(a). As can be observed in this

Fig. 4. Configurations adopted in the simulations.

figure, seven mesh blocks were used and five of them are multi-level nested, which means five blocks are nested in another, larger, nested mesh block. The number of cells for each block was in the following ratio: 0.22, 0.17, 0.03, 0.06, 0.11, 0.33 and 1, from mesh block 1 to 7, respectively. Three meshes were used to verify the achievement of grid convergence. These were 862,500 cells, 1,725,000 cells and 6,900,000 cells. The sequential finer grid was initialized by interpolating the previous calculated values onto the grid. Starting the new grid with the old values allowed the new solution to converge quicker. The smallest cell size for the finest grid used (6,900,000 cells) was approximately 3.2 mm.

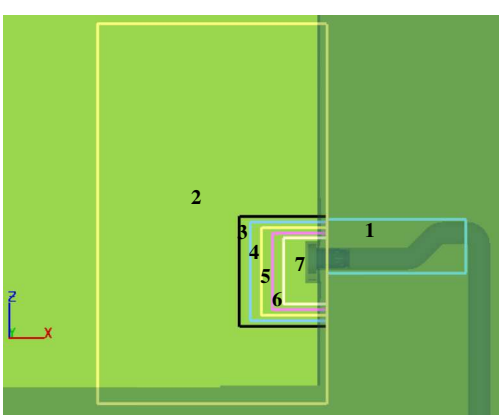


(a) *x*-*z* view of the multi-block mesh setup

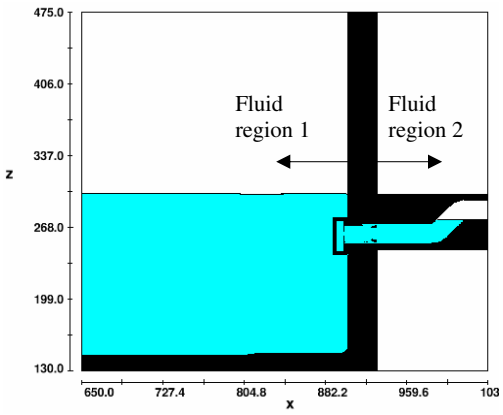


(b) Two fluid regions assumed as initial conditions in the simulations

Fig. 5.

### *Initial Conditions*

In the physical model [Fig. 3(a)], the type of flow from the manhole tank to the outflow pipe changed from pressurized to gravity flow at the downstream end. In the flow restrictor zone the flow was fully pressurized. In order to simulate this flow configuration, two fluid regions were specified initially [Fig. 5(b)]. For the first fluid region, the same water height as specified at the left boundary of mesh block 2 was imposed. For the second fluid region, a water height that fills partially (about 50%) the downstream end of the outflow pipe was imposed. If initially the outflow pipe is fully pressurized, the program converges to a solution in which the outflow pipe is fully pressurized. This solution is correct but corresponds to a different setup than the physical model.

## Results and Discussions

The experimental results for discharge coefficients and rating curves for the four positions [Fig. 3(b)] were very similar. Thus, in the numerical simulations only position 1 [Fig. 3(b)] was simulated. Fig. 6(a) presents a plot of $Q$ as a function of $H_t - H_v$ for the position 1 of the VFR with $L_s$ = 0 cm. The numerical simulations were performed using three different meshes to ensure the achievement of grid convergence. Because the results using the finest mesh (6,900,000 cells) and the intermediate mesh (1,725,000) were not close, two extra simulations using a mesh of 13,800,000 cells were performed. The results of these simulations for the rating curve (not presented in Fig. 6(a) for clarity) agreed within 1% with the ones obtained using a mesh of 6,900,000 cells. Thus, it can be said that grid convergence has been achieved using a mesh of 6,900,000 cells. As can be observed in Fig. 6(a), the numerical rating curve using a mesh of 6,900,000 cells (converged solution) have a good agreement with the experimental rating curve. The numerical rating curve using the converged solution agrees within 5% with the experimental rating curve.

The experimental discharge coefficient for the VFR for all positions (1-4) and for $L_s = 0$ cm is found to be 0.11 considering that the controlling cross-sectional area is the rectangular entrance to the VFR (72.58 cm$^2$). The numerical $C_d$ obtained using the converged solution was found to be 0.12. These results clearly show that the numerical discharge coefficient agree well with the one obtained from the experiments.

When no flow restrictor is installed, the flow discharges are much larger than the case when a VFR is installed. The experimental rating curve for the case of no flow restrictor is shown in Fig. 6(b). The flow discharge for a given head differential ($H_t - H_v$) when no restrictor is installed can be as large as 30 times of that when a VFR is installed. In other words, when using a VFR, the magnitude of the discharge for a given head differential can be as low as 3% of the discharge obtained if no restrictor is installed. For the case of no flow restrictor, the experimental and numerical discharge coefficient was found to be 0.76, which agrees well with the average value of $C_d$ = 0.75 published by Brater et al. (1996) for short tubes protruding into a reservoir. The results demonstrate that the inclusion of the helicoidal chamber and the series of contractions and expansions in a VFR increase the energy losses significantly as the flow is forced through a much more tortuous path and turbulence is increased due to shearing of the flow. Two visualizations of the flow inside the VFR are shown in Fig. 7.

As noted previously, the exact location of the upstream seal has a large influence on the

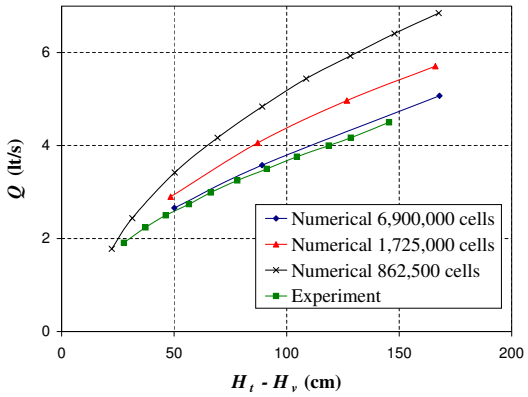


(a) Experimental and numerical rating curves for the VFR

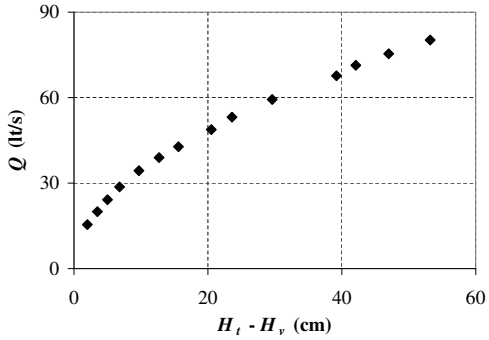


(b) Experimental rating curves when no VFR is installed

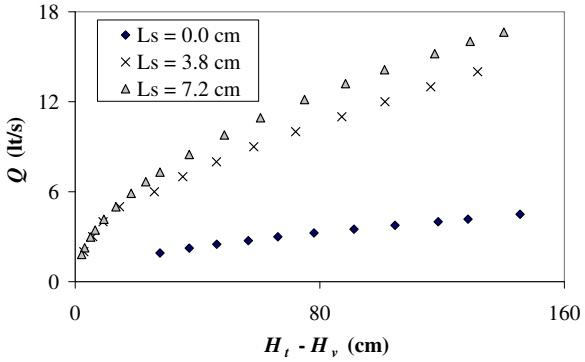


(c) Experimental rating curves for the VFR for various $L_s$

Fig. 6.

discharge coefficient for the flow restrictor. During preliminary comparison between experimental and numerical results, large differences were observed among the rating curves ($Q$ vs $H_t - H_v$) for the same conditions. Further examination determined that in the experiments the upstream seal had shifted, exposing the slats and providing an alternate flow path. Fig. 6(c) is a plot of the rating curves ($Q$ vs $H_t - H_v$) with the length of exposed slats ($L_s$) equal to 0 cm, 3.8 cm, and 7.2 cm. As demonstrated by the data, the position of the upstream seal has a significant impact on the discharge coefficient of the flow restrictor, $C_d$, with values ranging from 0.11 with $L_s$ = 0 cm to 0.44 with $L_s$ = 7.8 cm. This results in approximately a 400% increase in discharge between a correctly installed flow restrictor ($L_s$ = 0 cm) and an incorrectly installed restrictor. The discharge coefficient with $L_s$ = 3.8 cm is $C_d$ = 0.37, lying between the two extreme cases, as would be expected.

## Conclusions

This paper presents the results of a numerical and experimental study conducted for evaluating the effectiveness of a vortex flow restrictor in limiting peak flows. The key results are as follows:

(1) The use of vortex flow restrictors are effective at decreasing the magnitude of dis-

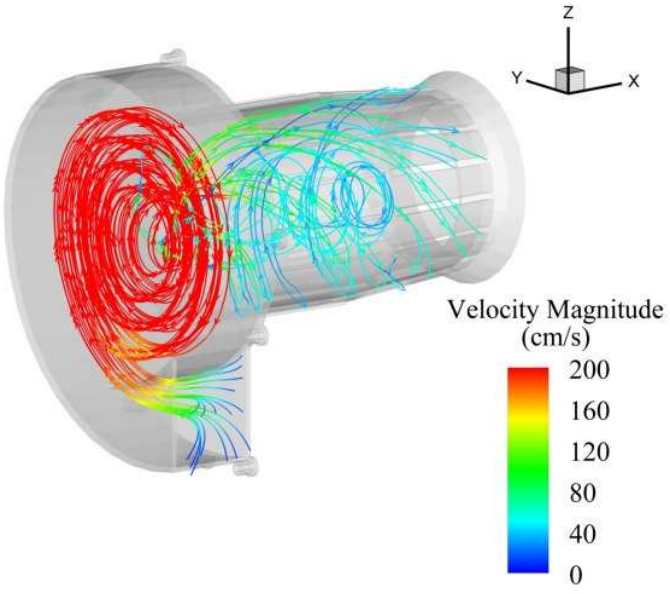


(a)

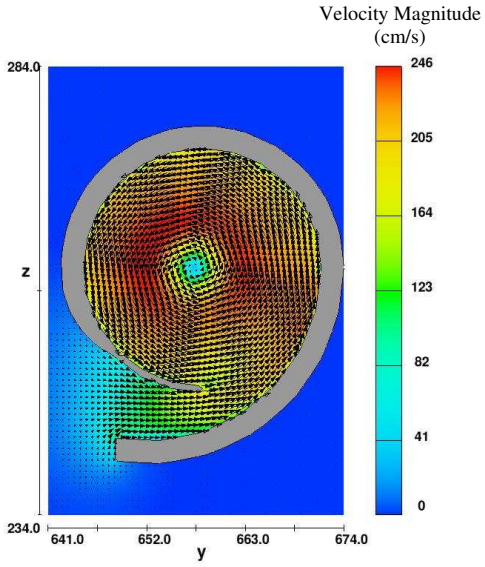


(b)

Fig. 7. Visualizations of the flow in the VFR

charges that enter a storm sewer pipe. When using this type of restrictor, the magnitude of the discharge for a given head differential can be reduced substantially compared to the case where no flow restrictor is in place. More research is needed.

(2) Special care must be exercised during the installation of vortex flow restrictors ensuring that the flow restrictor seals are positioned properly. Changes in the upstream seal position may result in an increase in the discharge of up to 400% with a similar increase of the discharge coefficient. The large change in the discharge coefficient can invalidate hydrologic and hydraulic models that rely on the assumption of a constant discharge coefficient.

(3) Complex flows such as the flow inside a VFR can be simulated accurately using numerical tools. Physical model studies still provide the basis to test numerical predictions. However, numerical methods may offer accurate solutions that supplement physical models and also provide more data, showing the entire discretized pressure and velocity fields.

## Acknowledgments

The authors gratefully acknowledge the Metropolitan Water Reclamation District of Greater Chicago for their support of this research as part of the TARP Modeling Project. The findings and opinions presented in this paper are solely those of the authors.

## References

Brater, E.F., King, H.W., Lindell, J.E., Wei, C.J. (1996). Handbook of Hydraulics (7th Ed.), McGraw Hill, New York.

Flow Science, Inc. (2005). FLOW-3D v. 9.0 user's manual, Flow Science, Inc., Santa Fe, N.M.

Hirt, C.W. (1992). "Volume-fraction techniques: Powerful tools for flow modeling." *Flow Sci. Rep*. FSI-92-00-02, Flow Science, Inc., Santa Fe, N.M.

Hirt, C.W., and Sicilian, J.M. (1985). "A porosity technique for the definition of obstacles in rectangular cell meshes." *Proc., 4th Int. Conf. Ship Hydro*., National Academy of Science, Washington, D.C., 119.

Nelson, K.D., Weber, L.J. (2000). "Submergence effects on the discharge coefficient for rectangular orifices." *Proc. 2000 Joint Conf. on Water Resourc. Eng. And Water Resourc. Planning and Management*, July 30-Aug 2 2000, Minneapolis.

Raasch, J.J. (2002). "Store sewer overflow control device." United States Patent. Patent No.: US 6,406,216 B1.

Rodi, W. (1980). "Turbulence models and their application in hydraulics." *International Association for Hydraulic Research*, Delft, The Netherlands, 2730.

Versteeg, H.K., and Malalasekera, W. (1995). An introduction to computational fluid dynamics, Longman Scientific and Technical, New York.